

## Fast imaging of laser-blow-off plume: Lateral confinement in ambient environment

Sony George,<sup>1</sup> Ajai Kumar,<sup>2,a)</sup> R. K. Singh,<sup>2</sup> and V. P. N. Nampoori<sup>1</sup>

<sup>1</sup>ISP, Cochin University of Science and Technology, Cochin 682 022, India

<sup>2</sup>Institute for Plasma Research, Gandhinagar 382 428, India

(Received 17 November 2008; accepted 10 March 2009; published online 7 April 2009)

The dynamics of plasma plume, formed by the laser-blow-off of multicomponent LiF-C thin film under various ambient pressures ranging from high vacuum to argon pressure of 3 Torr, has been studied using fast imaging technique. In vacuum, the plume has ellipsoidal shape. With the increase in the ambient pressure, sharp plume boundary is developed showing a focusing-like (confinement in the lateral space) behavior in the front end, which persists for long times. At higher ambient pressure ( $>10^{-1}$  Torr), structures are developed in the plasma plume due to hydrodynamic instability/turbulences. © 2009 American Institute of Physics. [DOI: 10.1063/1.3111441]

In recent times, the study of laser produced plasma interaction in ambient gas has received meticulous interest because of its vast applications including laser deposition, nanoparticle formation, cluster production, material science, and extreme ultraviolet lithography.<sup>1-4</sup> Neutral atomic beams (Li, C, Si, Ni) produced by laser-blow-off (LBO) technique are used in plasma diagnostics to measure edge plasma parameters or impurity transport in tokamak plasmas.<sup>5,6</sup> Comparison between the plume expansion in vacuum and ambient environment provides the knowledge of many physical processes such as deceleration, attenuation/enhancement of emission, thermalization of the ablated species, formation of shock waves, and plume oscillations.

In LBO,<sup>7</sup> the laser beam interacts with a thin film of target supported on a thick transparent substrate. The ablated material propagates along the direction of incident laser beam. The formation and expansion dynamics of LBO plume are discussed in detail in Refs. 8–10. Earlier studies based on emission spectroscopy have revealed the effects of ambient gas on LBO plume, without any details regarding the structure formation, size, and shape of the plume in various ambient environments.

In case of laser produced plasma from solid surface, plume focusing-like behavior was observed in the presence of ambient gas. Lichtenwalner *et al.*<sup>11</sup> reported focusing/narrowing of the ablated flux distribution from a lead zirconate titanate target as O<sub>2</sub> pressure increased from 10 to 300 mTorr and further increase in the pressure ( $\sim 900$  mTorr) results in plume broadening. The plume focusing is observed over a short spatial distance, which diverges out for longer distance. These plume narrowing or broadening regimes are both explained in terms of gas scattering effects. Shen *et al.*<sup>12</sup> reported the spatial confinement effects in Al plasma plume between a pair of Al-plate walls, due to the reflection and the compression of the shock wave.

The most realistic approach to explain the focusing of laser-produced plasma has been made by Bulgakov and Bulgakova.<sup>13</sup> They modeled the lateral confinement of the plume using simple gas-dynamic considerations based on the analogy between an ablated plume and a supersonic under-expanded gaseous jet expending into the background gas.

This model provides a basis for the focusing or narrowing of the plume, observed at fairly high laser fluence and ambient pressures and predicts focusing of plume over a short spatial region and thereafter diverging out.

It is worth mentioning that neutral species are the main constituents of the LBO plumes.<sup>9,14,15</sup> It also consists of the ions mostly in singly ionized stage.<sup>9,14</sup> Hence, it is worthwhile to study the interaction between background gas and LBO plume with regard to plume focusing and formation of structures due to hydrodynamic instability.

The fast photography of expanding visible plume emission, using a nanosecond gated intensified charged coupled device (ICCD), can provide information on the “local” structure, dynamics of the constituent particles, and geometrical aspects of the plume. In this paper we report the results obtained from fast photography of the LBO plume at different ambient pressures ranging from high vacuum to 3 Torr.

A detailed description of experimental setup has been reported in our previous papers.<sup>8,14</sup> The plasma is viewed through a quartz window mounted orthogonal to the direction of plume expansion. The time resolved images have been recorded by an ICCD camera having variable gain, gate time, and spectral response in 350–750 nm region. In the present experiment, the gate time is set to 4 ns. Length and full width at half maximum of the plume are estimated by segmentation algorithm. For better visibility, gray images have been converted into pseudocolored images using jet color map.

Spatio-temporal evolution of optical emission from the electronically excited plume species, driven by collisional processes between electrons, ions, and neutrals, is imaged by ICCD at different argon pressures ranging from  $10^{-5}$  to 3 Torr (Fig. 1). These images are recorded at a laser irradiance of  $\sim 3$  GW cm<sup>-2</sup>. For comparison, all the images (Fig. 1) are normalized to its maximum intensity. Following points are noted from the visual observation of the images.

After the termination of the laser pulse, the plume expands in the forward direction. In vacuum, the plume expands adiabatically and has an ellipsoidal shape. During the expansion, electron density reduces rapidly and hence the probability of electron impact excitation is also reduced. This leads to reduction in the emission intensity of the plume. For  $t > 1000$  ns, emission intensity is beyond the detection limit

<sup>a)</sup>Electronic mail: ajai@ipr.res.in.

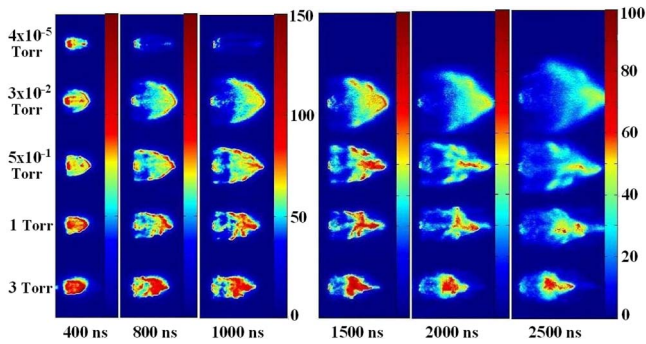


FIG. 1. (Color online) Gated ICCD images of the integrated emission from the expanding plasma plume for different time delays with respect to the plasma initiation. The integration time was fixed as 4 ns. The ambient gas pressure was varied from  $10^{-5}$  to 3 Torr.

of the ICCD due to lower dynamic range of the camera. It shows a three-line structure parallel to the plume expansion direction and is more intense at the leading edge of the plume and closer to the target.

The size, shape, and intensity of the plasma plume are completely modified with increase in ambient gas pressure. At  $10^{-2}$  Torr, plasma plume becomes wider and intense in comparison to that observed in vacuum. As shown in Fig. 1, a bright luminescence on the plume boundary (wakelike) is formed between plasma and ambient gas. Lifetime of the plume is also increased and it persists up to  $t > 2500$  ns after the plume initiation. At this pressure, interpenetration of the plasma plume and ambient gas occurs, which causes an increase in collision between the plume species and ambient gas.<sup>16,17</sup> Our estimation shows that at  $t \sim 400$  ns, plume expands in the collisional regime where the plume dimension ( $\sim 7$  mm) is greater than the mean free path ( $\sim 4.8$  mm at  $5 \times 10^{-2}$  Torr) of the ejected species. The increase in collision processes is responsible for the enhancement in the observed emission intensity due to the transfer of kinetic energy from plasma to the background gas via ion-ion Coulomb scattering, ion-neutral collisions, charge exchange interactions, etc. With the increase in the time delay, plume becomes more collisional and at  $t > 2500$  ns, plume species diffuse into the background gas. It is worth to mention here that at a distance of 4 mm from the target (corresponding to  $t > 300$  ns), enhancement in emission intensity is more pronounced for Li I in comparison to Li II.<sup>9</sup>

As the background pressure is further increased to  $3 \times 10^{-1}$  Torr, the plume appears compressed (lateral direction) when compared to that at  $10^{-2}$  Torr. It can be clearly observed that a sharp boundary is also formed around the expanding plume. At this pressure, interpenetration of the plume species and background gas is relatively weak.<sup>17</sup> The plume material is pushed more against the expansion resulting in the formation of a layer of compressed gas around the plume.

A closer examination of plume structure at pressure  $\geq 10^{-1}$  Torr reveals that the effect of background gas is more pronounced in the lateral direction than in the direction of expansion. A narrow stream of dense emission is observed along the centerline of the plume, which propagates like free expansion in vacuum. This can be explained as follows. The results from optical emission spectroscopy<sup>9,10,14</sup> have shown that LBO plume consists of fast and slow components formed by two different mechanisms. Due to higher translation energy, energetic fast component of plume penetrates

into the ambient gas with little interaction and therefore has same velocity as in vacuum. The slow component of the plume (lateral part) undergoes gas hydrodynamic effect resulting in nonlinear expansion in the ambient environment.

At pressure  $\geq 10^{-1}$  Torr, the internal structure (breaking of image at the edge) in the plume starts appearing. Center portion of the plasma plume is almost unchanged whereas internal structure due to turbulence is observed at the edge of the plasma. This edge turbulence is observed right from 400 ns and  $3 \times 10^{-1}$  Torr. This effect gets more pronounced with increasing time delay and ambient pressure. For  $\geq 1$  Torr, the ambient gas penetrates and leads to collisions inside the plume. This results in the generation of complex internal structure inside the plume.

As stated earlier, for  $\sim 10^{-1}$  Torr, the interpenetration between the plume material and ambient gas is restricted and an interface is formed. This indicates that contact boundary instability begins to appear during plume expansion at this pressure. Therefore, there is a finite probability of development of hydrodynamical instabilities e.g., Rayleigh-Taylor (RT) instability during the expansion.

Due to RT instability, the interface between the expanding plume and ambient gas gets perturbed. We have estimated the background gas density at 400 ns, which produces the RT instability using the relation,<sup>18</sup>  $\rho_b = 3m / (4\pi R^3)$ , where  $m$  is the mass of the ablated material and  $R$  is the plume dimension. In the present case, the mass of the ablated material is  $0.992 \mu\text{g}$ . At 400 ns, the measured plume length is 7.3 mm. Using these parameters the estimated density of the background gas comes out to be  $0.609 \mu\text{g}/\text{cm}^3$ , which corresponds to a pressure of  $\sim 2.8 \times 10^{-1}$  Torr. This is in agreement with the beginning of turbulence at  $3.0 \times 10^{-1}$  Torr. On the basis of the above analysis, we can say that RT instability should be responsible for the observed structure.

In order to explain the plume expansion dynamics in a different gas environment, we have studied the plume length versus time (Fig. 2). The linear dependence of the time with the plume length in vacuum suggests the free expansion of plasma plume as evident from Fig. 2(a). It is observed that initially ( $< 1000$  ns), the plume velocity is almost independent of the ambient pressure and follows vacuum-like expansion. After that, it experiences resistive force from the background gas. At lower ambient pressure, slowing down of ejected species can be treated under the classical drag force model.<sup>19</sup> For gas pressure of  $10^{-2}$  Torr, the plume image data fit reasonably well with the drag force model  $z = z_f [1 - \exp(-\beta t)]$  [Fig. 2(b)], where  $\beta$  is the slowing coefficient and  $z_f$  is the stopping distance of the plume. The best fitting gives  $\beta = 3.8 \times 10^5/\text{s}$  and  $z_f = 5.6$  cm. On the other hand, at relatively high pressures ( $\geq 1$  Torr), where the ablated mass is small compared to the mass of the background gas in motion, the formation of a shock front<sup>20</sup> could be observed. In the present case with 3 Torr argon pressure, the plume followed  $R \propto t^{0.72}$  agreeing well with the shock model [Fig. 2(c)].

For better understanding of the effect of ambient environment on the two dimensional shape of the plume, we have plotted the aspect ratio (length/width) as a function of time delay (Fig. 3). Up to 1000 ns, plasma plume is nearly hemispherical (width  $\sim$  length) for the  $10^{-2}$  Torr. The aspect ratios attain saturation for  $t \geq 1000$  ns at 3 Torr indicating gas

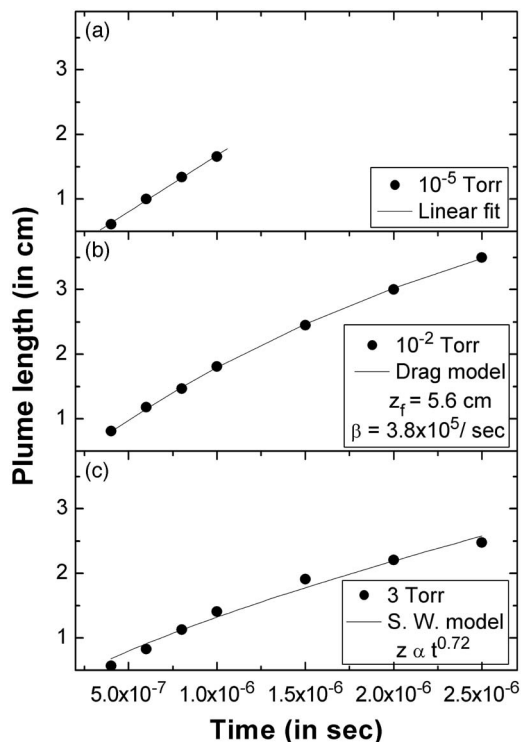


FIG. 2. Plume length vs time plots for the observed images for three different ambient environments (a) vacuum, (b)  $10^{-2}$  Torr, and (c) 3 Torr of argon gas. The solid line represents the best fit of the experimental data in accordance with the linear fit, drag model, and shock wave model for the ambient pressures  $10^{-5}$ ,  $10^{-2}$ , and 3 Torr, respectively.

pressure restricts the lateral as well as forward motion of the plume species in the same proportion.

One of the most important observations of the present experiment is the strong focusing (lateral confinement) of the LBO plume, which persists for longer times. We do not observe any divergence of plume up to a time delay of  $3.5 \mu\text{s}$  and 3 Torr pressure. The strength of the focusing depends on the time delay and ambient pressure. These observations are quite different from the earlier reports for the plume confinement/focusing. Similar focusing pattern is also observed in the sequence of images recorded with an interference filter ( $\lambda_0=670.8 \text{ nm}$ ; FWHM  $\sim 1 \text{ nm}$ ) corresponding

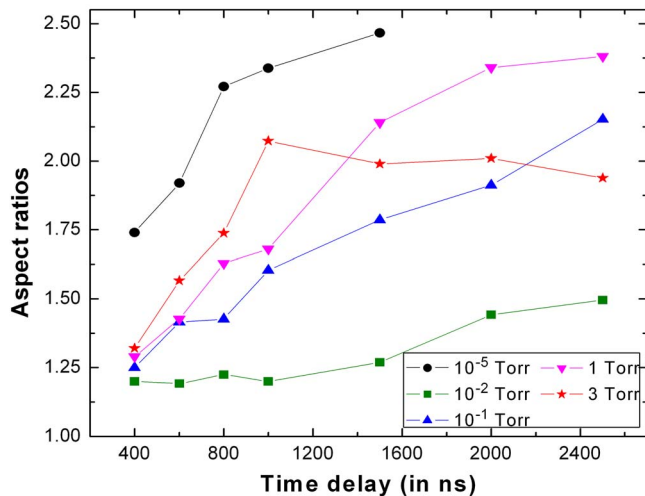


FIG. 3. (Color online) Aspect ratios (length/width) of the plume as a function of time delay and ambient gas pressure.

to the neutral lithium line in front of ICCD camera. This also indicates that plume focusing is a gas hydrodynamic phenomenon.

However, the strong LBO plume focusing and its existence at farther spatial positions remain unexplained by earlier proposed model.<sup>13</sup> Therefore, we feel that more theoretical and experimental investigations are required to explain the plume focusing in terms of atomic physics and hydrodynamics.

In summary, the behavior of the plasma plume has been found strongly influenced by the background gas pressure. We observe that the shape of the plume is ellipsoidal in vacuum with a three-line structure parallel to the plume direction. The plume shape has maximum size at  $10^{-2}$  Torr. For  $>10^{-2}$  Torr the plume starts confining in lateral direction. A strong focusing effect is reported. The observed focusing effect persists for a longer time ( $>2500 \text{ ns}$ ) and higher pressure ( $>3 \text{ Torr}$ ) without any noticeable divergence. Further, at high background pressures, it has been found that RT instability is responsible for the turbulence on the edge regions.

Result shows that the neutral species also follow the focusing phenomena, which confirms that plume focusing is due to gas hydrodynamics. Further work is in progress to understand plume focusing and formation of structures in the plume.

Sony George acknowledges UGC for research fellowship (RFSMS) and also IPR for the support and permission given to pursue this work.

- <sup>1</sup>D. B. Chrisey and G. K. Hubler, *Pulsed Laser Deposition of Thin Films* (Wiley, New York, 1994).
- <sup>2</sup>D. B. Geohegan, A. A. Puretzky, G. Duscher, and S. J. Pennycook, *Appl. Phys. Lett.* **73**, 438 (1998).
- <sup>3</sup>H. W. Kroto, J. R. Heath, S. C. O'Brien, R. F. Curl, and R. E. Smalley, *Nature (London)* **318**, 162 (1985).
- <sup>4</sup>M. Masnavi, M. Nakajima, A. Sasaki, E. Hotta, and K. Horioka, *Appl. Phys. Lett.* **89**, 031503 (2006).
- <sup>5</sup>A. Pospieszczyk, F. Aumayr, E. Hintz, and B. Schweer, *J. Nucl. Mater.* **162**, 574 (1989).
- <sup>6</sup>T. Parisot, R. Guirlet, C. Bourdelle, X. Garbet, N. Dubuit, F. Imbeaux, and P. R. Thomas, *Plasma Phys. Controlled Fusion* **50**, 055010 (2008).
- <sup>7</sup>F. J. Adrian, J. Bohandy, B. F. Kim, A. N. Jette, and P. Thomson, *J. Vac. Sci. Technol. B* **5**, 1490 (1987).
- <sup>8</sup>A. Kumar, V. Chaudhari, K. Patel, S. George, S. Sunil, R. K. Singh, and R. Singh, *Rev. Sci. Instrum.* **80**, 033503 (2009).
- <sup>9</sup>R. K. Singh, A. Kumar, B. G. Patel, and K. P. Subramanian, *J. Appl. Phys.* **101**, 103301 (2007).
- <sup>10</sup>R. K. Singh, A. Kumar, V. Prahlad, and H. C. Joshi, *Appl. Phys. Lett.* **92**, 171502 (2008).
- <sup>11</sup>D. J. Lichtenwalner, O. Auciello, R. Dat, and A. I. Kingon, *J. Appl. Phys.* **74**, 7497 (1993).
- <sup>12</sup>X. K. Shen, J. Sun, H. Ling, and Y. F. Lua, *Appl. Phys. Lett.* **91**, 081501 (2007).
- <sup>13</sup>A. V. Bulgakov and N. M. Bulgakova, *J. Phys. D* **31**, 693 (1998).
- <sup>14</sup>A. Kumar, R. K. Singh, V. Prahlad, and H. C. Joshi, *J. Appl. Phys.* **104**, 093302 (2008).
- <sup>15</sup>J. F. Friichtenicht, *Rev. Sci. Instrum.* **45**, 51 (1974).
- <sup>16</sup>S. Harilal, C. V. Bindhu, M. S. Tillack, F. Najmabadi, and A. C. Gaeris, *J. Appl. Phys.* **93**, 2380 (2003).
- <sup>17</sup>S. Amoroso, B. Toftmann, J. Schou, R. Velotta, and X. Wang, *Thin Solid Films* **453**, 562 (2004).
- <sup>18</sup>R. Betti, V. N. Goncharov, R. L. McCrory, and C. P. Verdon, *Phys. Plasmas* **5**, 1446 (1998).
- <sup>19</sup>J. C. S. Kools, *J. Appl. Phys.* **74**, 6401 (1993).
- <sup>20</sup>W. K. A. Kumuduni, Y. Nakayama, Y. Nakata, T. Okada, and M. Meada, *J. Appl. Phys.* **74**, 7510 (1993).